


Optimization of iron and manganese removal from groundwater using activated carbons derived from waste materials via response surface methodology

Deiaa Wafa^{1*} , Abd-Elaziz El-Sayed¹, Mohamed Ayoub¹, Ahmed El-Morsy¹

¹ Public Works Engineering Department, Faculty of Engineering, Tanta University, Tanta, 31511, Egypt

* Corresponding author's e-mail: deiaa152577@f-eng.tanta.edu.eg

ABSTRACT

Activated carbon derived from cigarette butts (CI-AC), corn cobs (CO-AC), and luffa sponge (LU-AC) was evaluated for adsorbing iron and manganese from aqueous solutions. Each material was carbonized at 300 °C for 2 hours, followed by chemical activation with HCl (carbonaceous material/HCl ratio of 1:5). Fourier transform infrared spectroscopy characterized the adsorbents. The effects of pH, adsorbent dosage, initial Fe and Mn concentrations, and contact time on Fe(II) and Mn(II) adsorption were investigated using response surface methodology (RSM) based on a Box–Behnken design. Optimal conditions for CI-AC were: pH 8, 50 minutes contact time, 2 g adsorbent dose, and 3.32 mg/l initial Fe and Mn concentration, resulting in 70.33% Fe and 65.12% Mn removal. Optimal conditions for CO-AC were: pH 6.34, 37.8 minutes contact time, 1.25 g adsorbent dose, and 3.52 mg/l initial Fe and Mn concentration, resulting in 88.53% Fe and 79.75% Mn removal. Optimal conditions for LU-AC were: pH 6.49, 50 minutes contact time, 1.67g adsorbent dose, and 0.5 mg/l initial Fe and Mn concentration, resulting in 79% Fe and 86.37% Mn removal.

Keywords: adsorption, FTIR, groundwater, iron and manganese, RSM.

INTRODUCTION

Groundwater resources are critical for developing safe and sufficient drinking water supplies worldwide (Thinojah and Ketheesan, 2022). In Egypt, fresh groundwater resources contribute to less than 20% of the total potential of water resources. Groundwater is an essential source of drinking water in Egypt, especially in areas with limited or unreliable surface water resources. It plays a vital role in providing potable water to rural and urban populations, particularly in the desert and remote areas of Egypt (Overview, 2016). Iron and manganese are two metals frequently detected in well water, often due to the presence of a stony bed in the groundwater, leading to an overabundance of metallic taste and stains (Akbar et al., 2016; Zadeh et al., 2022). In Egypt, the most frequent issue preventing the usage of groundwater is its high iron and/or

manganese level (Mahmoud et al., 2014). Iron and manganese may provide an unpleasant taste, odor, and color to water. Iron stains clothes, porcelain, plates, cutlery, glassware, sinks, fixtures, and concrete reddish-brown. Manganese is responsible for brownish-black stains. Deposits of iron and manganese form in pipes, pressure tanks, water heaters, and water softening devices. These deposits obstruct the passage of water and lower the pressure.

Various techniques can be employed to remove iron (Fe) and manganese (Mn) from groundwater, including aeration oxidation, ion exchange membrane processes, biological filtration, adsorption, coagulation, filtration, and chemical precipitation (Barloková and Ilavský, 2010; Matouq et al., 2015). Coagulation and chemical precipitation are effective but tend to use large amounts of chemicals and generate sludge containing metals that requires further treatment. Methods such as

membrane filtration, ion exchange, reverse osmosis, and oxidation-reduction are less commonly used due to issues like high costs, significant energy demands, and membrane fouling (Mani and Kumar, 2014; Zhao et al., 2016).

Among these, adsorption is considered one of the most promising techniques because of its simplicity, cost-effectiveness, efficiency, environmental friendliness, and the wide availability of suitable materials (Wang et al., 2009). The success of the adsorption process largely depends on the type of adsorbent employed. Recently, there has been increased interest in low-cost adsorbents derived from agricultural waste, industrial by-products, or natural polymers, which are gaining popularity in the removal of heavy metals (Anastopoulos et al., 2019). This research aims to evaluate how effectively adsorption can remove iron (Fe) and manganese (Mn) from contaminated groundwater. It investigates the impact of various operational factors, including contact time, initial concentrations of Fe and Mn, pH, and the dose of adsorbent used, on the treatment performance. Additionally, the study details the preparation of activated carbon from agricultural and household waste materials such as cigarette butts, corn cobs, and luffa sponge.

MATERIALS AND METHODS

Materials and chemicals

Smoked cigarette butts were collected from cafes and employees' offices. Corn cobs were collected from a farm in a village in Talkha, Dakahlia Governorate. A luffa sponge was purchased from the market in Talkha city. Hydrochloric acid with a 32% concentration was used to activate different types of adsorbents. Filter paper, size 9.0 cm, 102 qualitative, 8 microns pore size, was used. These chemical materials were sourced from Al-Gomhoria Company for Chemical Supplies, Egypt. The pH level of the solution was adjusted using hydrochloric acid (HCl) and sodium hydroxide (NaOH) purchased from Al-Gomhoria Company for Chemical Supplies in Egypt.

Preparation of Fe (II) and Mn (II) stock solutions

Iron (II) and manganese (II) solutions, ranging from 0.5 mg/L to 7.0 mg/L, were prepared

by diluting stock solutions of ferric nitrate ($\text{Fe}(\text{NO}_3)_3$) and manganese nitrate ($\text{Mn}(\text{NO}_3)_2$) with distilled water. All analytical grade chemicals were sourced from Sigma Aldrich - Supelco Analytical Products (Germany).

Preparation of activated carbon

Cigarette butts activated carbon (CI-AC)

Smoked cigarette butts were removed from their wrapping and washed with distilled water to eliminate soot and tobacco contamination. The washed butts were then dried at 105 °C until a constant weight was achieved. Carbonization was performed by placing the dried butts in a porcelain dish within a muffle furnace at 300 °C for 2 hours under an argon atmosphere. The resulting carbon was removed, crushed, and sieved through a 90-mesh sieve. Activation was carried out by mixing the carbon with a 32% HCl solution (cigarette butts/HCl mass ratio of 1:5) and stirring at 150 RPM for 1 hour, followed by a 24-hour soak. The activated carbon was then vacuum-filtered using 9.0 cm filter paper (102 qualitative, 8 microns pore size), washed with distilled water until neutral pH was reached, dried at 105 °C for 3 hours, cooled, and stored in a desiccator, as shown in Figure 1a.

Luffa sponge (LU-AC) and corn cobs activated carbon (CO-AC)

Luffa activated carbon (LU-AC) was prepared by cutting luffa into small pieces, washing them with distilled water to remove contaminants, and then drying, carbonizing, and activating them using the same process as for cigarette butts activated carbon. Corn cobs activated carbon (CO-AC) was prepared as described for LU-AC, as illustrated in Figure 1b and 1c.

Adsorbents characterization

Fourier transform infrared spectroscopy (FT-IR) was used to characterize the functional groups of each adsorbent (CI-AC, LU-AC, and CO-AC). FT-IR spectra were acquired using a Bruker FT-IR spectrometer (Invenio S, Germany) with a spectral resolution of 4 cm^{-1} , 64 scans, and a wavenumber range of 400–4000 cm^{-1} (El-Haddad, 2013, 2020). This technique identifies materials by analyzing their molecular vibrations based on absorption peaks.

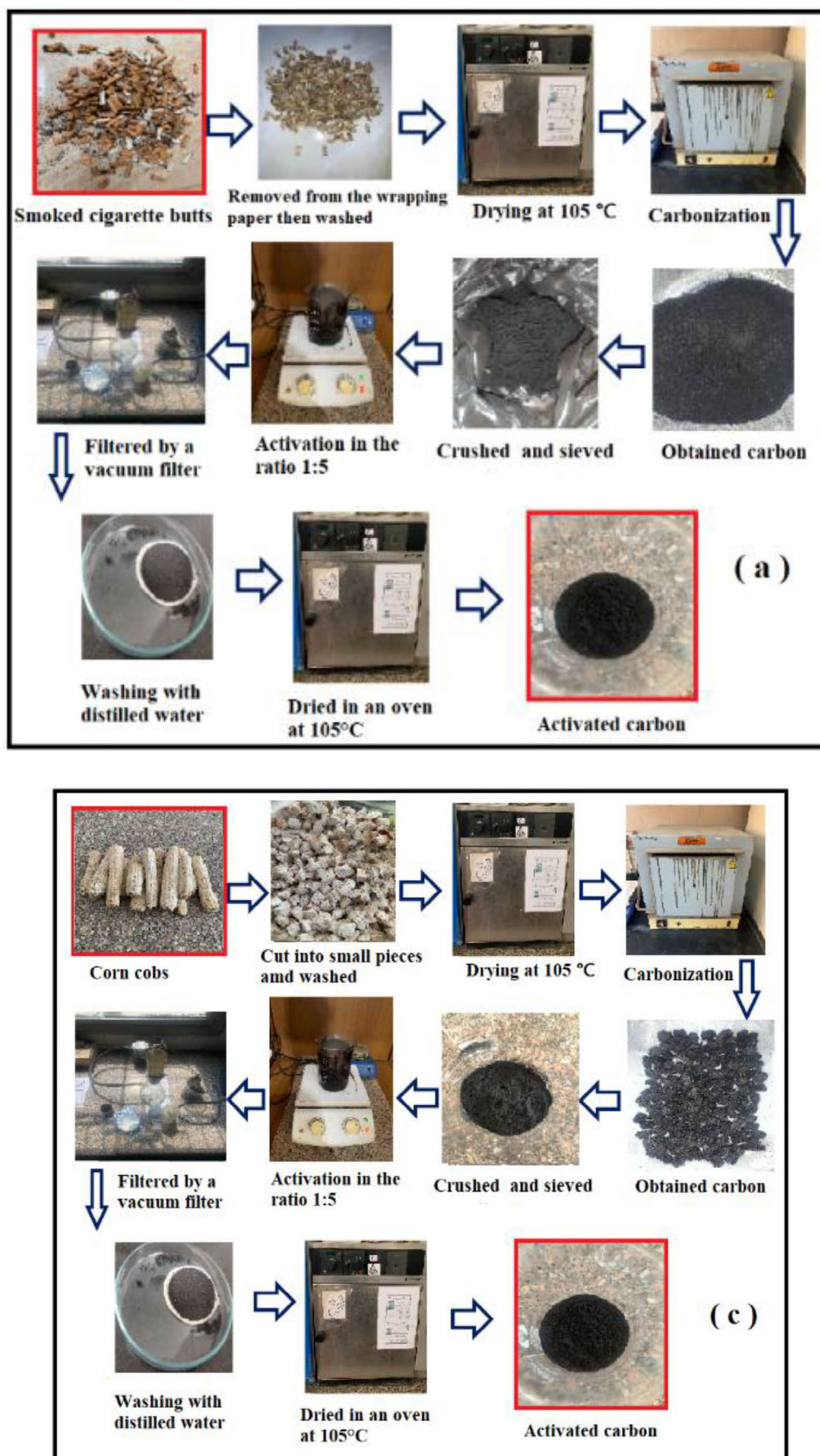


Figure 1. A schematic diagram of the experimental set up for the preparation of (a) CI-AC, (b) LU-AC and (c) CO-AC



Figure 1. Cont. A schematic diagram of the experimental set up for the preparation of (a) CI-AC, (b) LU-AC and (c) CO-AC

Experimental design using response surface methodology (RSM)

The Box-Behnken model (BBM), a response surface design suitable for experimental studies with more than two factors (Pereira et al., 2021), was used to develop experimental protocols and obtain a second-order mathematical model in the form of a quadratic polynomial equation.

$$y = \beta_0 + \sum_{i=1}^k \beta_i x_i + \sum_{i=1}^k \beta_{ii} x_i^2 + \sum_{i=1}^k \sum_{j=1}^k \beta_{ij} x_{ij} + \varepsilon \quad (1)$$

The response (y) was modeled using an equation incorporating an intercept (β_0), main effect coefficients (β_i), interaction effect coefficients (β_{ij}), second-order terms (β_{ii}), and a random error component (ε) determined by fitting the model to the data (Singh et al., 2005). Each operational variable was assessed at three values. Table 1 details the input parameters used to generate the experimental matrix.

Adsorption experiments were conducted for each adsorbent type (corn cob, luffa sponge, and cigarette butts) following a response surface

methodology (RSM) experimental design in Minitab 18. Experiments involved mixing a specific amount of each adsorbent with 100 mL of aqueous solution in a 250 mL glass beaker, followed by mechanical stirring at 150 rpm at room temperature (24–29 °C) for a set contact time. The effects of pH (2, 4, and 6), adsorbent dosage (0.2, 1.1, and 2 g/L), initial metal ion concentration (0.5, 3.75, and 7 mg/L), and contact time (10, 30, and 50 min) on the removal of Fe(II) and Mn(II) were studied.

Table 1 presents the upper and lower bounds of the independent variables. Following adsorption, the solution was filtered through 9.0 cm filter paper (102 qualitative, 8 µm pore size) using vacuum filtration to separate the adsorbents. The concentration of remaining Fe(II) and Mn(II) ions in the filtrate was then analyzed using an atomic absorption spectrometer (Varian AA240FS). The percentage removal of Fe and Mn from the aqueous solution was calculated using Equation 2.

$$\text{Removal efficiency (\%)} = \frac{(C_o - C_e)}{C_o} \times 100 \quad (2)$$

where: C_o – initial concentration of Fe or Mn (mg/L), C_e – final concentration of Fe or Mn (mg/L).

Table 1. Experimental matrix for RSM Box-Behnken design

N	Variable	Unit	-1	0	+1
X1	Adsorbent dose	(gm)	0.2	1.1	2
X2	pH	-	4	6	8
X3	Contact time	(min)	10	30	50
X4	Fe, Mn Initial Con	(mg/L)	0.5	3.75	7

Analytical methods

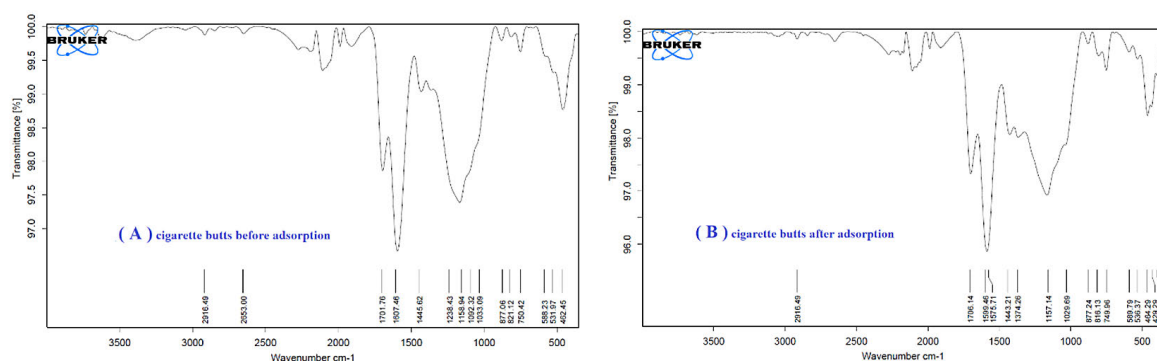
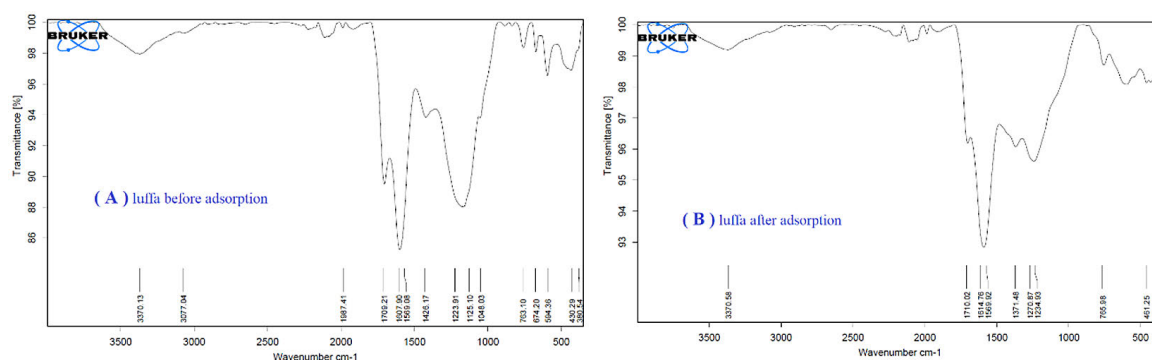
Iron and manganese analysis was conducted using a Varian Australia AA240FS atomic absorption spectrometer. Solution pH was measured and adjusted with a VWR Symphony SB70P pH meter. A Bruker Invenio S FT-IR spectrometer was used to identify functional groups in organic compounds.

RESULTS AND DISCUSSION

Adsorbents characterization by Fourier transform infrared spectroscopy (FTIR) analysis

FTIR spectra (Figures 2–4) revealed predicted peaks for CI-AC, LU-AC, and CO-AC before and

after iron and manganese adsorption. Comparison of the spectra (Table 2) showed shifts, disappearances, and new peaks following adsorption, indicating the involvement of various functional groups in the process (Krishni et al., 2014). Consistent with (Su et al., 2010) and (Nandiyanto et al., 2023), CO-AC exhibited the highest adsorption efficiency, likely due to strong O–H, C–O, and C=O groups, and potential metal–oxygen bonds, making it effective for polar, organic, and heavy metal pollutants. LU-AC showed moderate performance with O–H, C=O, and C≡N groups, suitable for polar contaminants but limited by the absence of strong C–O bonds. CI-AC had the weakest adsorption potential due to the lack of hydroxyl groups and weaker C=O and C–O functionalities, resulting in limited surface reactivity.

**Figure 2.** FTIR spectrum of (CI-AC): (A) before adsorption, (B) after adsorption Fe and Mn**Figure 3.** FTIR spectrum of (LU-AC): (A) before adsorption, (B) after adsorption Fe and Mn

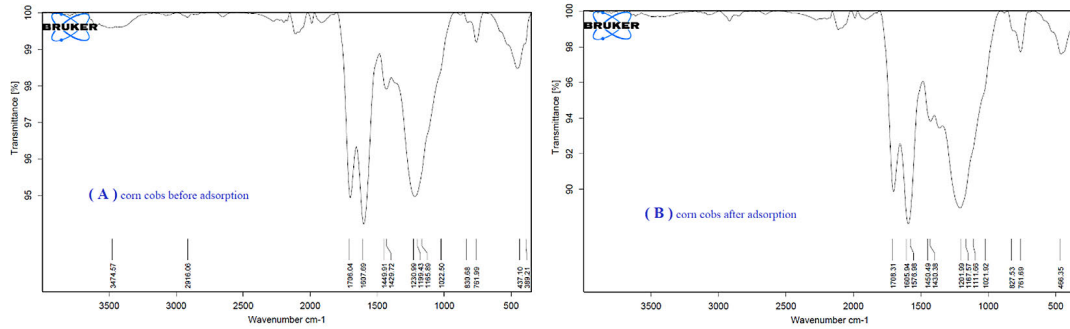


Figure 4. FTIR spectrum of (CO-AC): (A) before adsorption, (B) after adsorption Fe and Mn

Table 2. FTIR spectra of the CI-AC, LU-AC and CO-AC before and after adsorption

Wave number (cm ⁻¹)						Functional groups
Before	After	Before	After	Before	After	
(CI-AC)	(CI-AC)	(LU-AC)	(LU-AC)	(CO-AC)	(CO-AC)	
2916	2916	3370	3370.58	3474	-	C-H and O-H
1701	1706	3077	-	2916	2916.5	C=O and C-H
1607	1600	2987	-	1706	1708	C=C, C-H and C=O
-	1575	2709	-	1607	1605	N-H, C=C and C-H
1445	1443	1763	1710	-	1576	C-H, C=O and N-H
1374	1374	1674	1615	1449,1429	1450,1430	CH3, C=O and C-H
1238-1033	1157-1029	1594	1615	1231-1165	1202,1167, 1111	C-O and C=C
877	877	1430	1570	827,761	1570	C-H
-	816, 750	1380	1371	437	466	C-H and CH3
588,532, 462	590,536, 464,429, 392	-	1270–1234			Metal-Oxygen Bonds and C-O
		2223–2125	-			C=N or C=C
		-	461			C=N

Optimization of iron and manganese removal efficiency

Iron and manganese removal efficiencies (R%) for cigarette butts, corn cobs, and luffa sponge are presented in Tables 3, 4, and 5, respectively. Polynomial equations Equations 3–4 for cigarette butts, 5–6 for corn cobs, and 7–8 for luffa sponge derived using Minitab®18 software illustrate the relationship between variables and removal percentages.

$$R1 (Fe R\% \text{ by cigarette butts}) = 48.7 + 10.9X_1 - 0.635X_2 + 0.93X_3 - 5.35X_4 - 1.121X_1 \times X_1 - 0.00060X_2 \times X_2 - 1.72X_3 \times X_3 - 0.0800X_4 \times X_4 + 0.0718X_1 \times X_2 + 0.181X_1 \times X_3 + 0.538X_1 \times X_4 + 0.0297X_2 \times X_3 + 0.0535X_2 \times X_4 + 0.841X_3 \times X_4 \quad (3)$$

$$R2 (Mn R\% \text{ by cigarette butts}) = 17.56 + 6.77X_1 - 0.108X_2 - 9.99X_3 + 3.955X_4 - 0.059X_1 \times X_1 + 0.00204X_2 \times X_2 + 1.703X_3 \times X_3 + 0.0519X_4 \times X_4 + 0.0226X_1 \times X_2 + 0.432X_1 \times X_3 - 0.9021X_1 \times X_4 - 0.0102X_2 \times X_3 - 0.0125X_2 \times X_4 + 1.300X_3 \times X_4 \quad (4)$$

$$R3 (Fe R\% \text{ by corn cobs}) = 13.23 + 13.04X_1 + 1.076X_2 + 17.65X_3 + 4.158X_4 - 1.029X_1 \times X_1 - 0.00978X_2 \times X_2 - 5.132X_3 \times X_3 - 0.4744X_4 \times X_4 - 0.0153X_1 \times X_2 - 0.031X_1 \times X_3 - 0.0423X_1 \times X_4 - 0.1994X_2 \times X_3 - 0.109X_2 \times X_4 + 0.061X_3 \times X_4 \quad (5)$$

$$R4 (Mn R\% \text{ by corn cobs}) = -34.7 + 22.77X_1 + 1.627X_2 + 2.38X_3 + 2.11X_4 - 0.982X_1 \times X_1 - 0.00346X_2 \times X_2 - 1.39X_3 \times X_3 - 0.290X_4 \times X_4 - 0.2177X_1 \times X_2 - 0.659X_1 \times X_3 + 0.012X_1 \times X_4 + 0.1468X_2 \times X_3 - 0.0346X_2 \times X_4 + 0.673X_3 \times X_4 \quad (6)$$

$$R5 (Fe R\% \text{ by luffa}) = 36.73 + 2.11X_1 - 0.120X_2 + 11.62X_3 + 7.218X_4 - 0.002X_1 \times X_1 + 0.00478X_2 \times X_2 + 0.312X_3 \times X_3 + 0.0081X_4 \times X_4 - 0.0072X_1 \times X_2 + 0.802X_1 \times X_3 - 0.3912X_1 \times X_4 - 0.0305X_2 \times X_3 - 0.0239X_2 \times X_4 - 3.849X_3 \times X_4 \quad (7)$$

$$\begin{aligned}
 R6 (Mn\ R\% \text{ by luffa}) = & \\
 & -30.7 + 24.26 X_1 - 0.192 X_2 + \\
 & + 53.55 X_3 + 4.55 X_4 - 1.565 X_1 \times \\
 & \times X_1 - 0.00031 X_2 \times X_2 - 9.37 X_3 \times \\
 & \times X_3 - 0.6293 X_4 \times X_4 + 0.0406 X_1 \times \\
 & \times X_2 - 3.67 X_1 \times X_3 + 0.122 X_1 \times \\
 & \times X_4 - 0.0222 X_2 \times X_3 - 0.0052 X_2 \times \\
 & \times X_4 - 1.56 X_3 \times X_4
 \end{aligned} \quad (8)$$

where: X_1 (pH), X_2 (contact time), X_3 (adsorbent dose), X_4 (Fe, Mn initial concentration).

The observed and predicted iron and manganese removal efficiencies of cigarette butts, corn cobs, and luffa sponge activated carbon were highly similar (Tables 3–5). Response surface analysis showed high significance for each adsorbent material, with R^2 values of 94.44, 98.75, 95.07, 94.87, 98.13, and 98.89 for R1, R2, R3, R4, R5, and R6, respectively. Tables 6–8 show ANOVA results for iron removal efficiency (R1, R3, R5) and manganese removal efficiency (R2, R4, R6) using cigarette butts, corn cobs, and luffa sponge, respectively. Significant model restrictions for all adsorbents are indicated by small P-values and high F-values. Figures 5–7 show Pareto charts generated using Minitab®18, displaying the percentage of iron and manganese removal achieved by each adsorbent for

each operating model. Pareto chart analysis (Figure 5a) indicates that pH (A) and adsorbent dose (C) are the primary factors affecting Fe removal by cigarette butt activated carbon, followed by the interaction between contact time and Fe/Mn concentration (BD). Factors B and BB have minimal influence. Similarly, Figure 5b shows that pH is the most critical factor for manganese removal by cigarette butt activated carbon, followed by contact time and the interaction of pH with Fe/Mn concentration. Pareto analysis (Figure 6a and 6b) indicates that contact time (B) and pH (A) are the primary factors influencing Fe and Mn removal by corn cob activated carbon, followed by adsorbent dose (C) and initial Fe/Mn concentration (D). Pareto chart analysis (Figure 7a and 7b) indicates that pH (A) and adsorbent dose (C) are the primary factors affecting Fe and Mn removal, followed by initial iron and manganese concentration (D) and contact time (B).

Interaction analysis of factors in iron and manganese removal using cigarette butts, corn cobs, and luffa sponge activated carbon

Three-dimensional and contour plots Figures 8, 10, and 12 for iron removal (R%) and Figures

Table 3. Independent variables and the observed and predicted values of Fe and Mn removal efficiencies by (CI-AC)

No	PH	Time	Adsorbent dose	Fe, Mn IN concentration	R1% observed	R1 % predicted	R2 % observed	R2 % predicted
1	6	50	2	3.75	69.85	69.06	57.13	55.62
2	6	30	0.2	0.5	67.34	67.48	56.56	56.48
3	4	10	1.1	3.75	63.14	63.28	43.58	43.51
4	8	30	1.1	7	70.23	69.88	53.36	53.6
5	6	30	2	0.5	66.50	66.64	50.6	50.52
6	8	10	1.1	3.75	64.61	64.75	57.09	57.02
7	6	50	0.2	3.75	65.33	64.32	55.5	54.95
8	4	30	1.1	7	57.69	55.54	50.02	50.02
9	6	50	1.1	0.5	64.09	64.46	53.97	55.42
10	6	10	1.1	7	62.54	63.60	52.68	51.83
11	8	30	0.2	3.75	64.18	64.1	59.04	58.75
12	4	30	0.2	3.75	55.67	57.39	45.04	44.99
13	8	30	2	3.75	68.98	68.69	61.08	61.74
14	4	30	2	3.75	59.17	60.69	43.97	44.87
15	6	30	1.1	3.75	68.64	68.64	51.51	51.51
16	6	50	1.1	7	68.74	70.17	53.12	53.73
17	4	30	1.1	0.5	65.02	63.8	39.19	38.41
18	8	30	1.1	0.5	63.57	64.15	65.98	65.46
19	6	10	2	3.75	69.24	68.67	52.92	52.93
20	6	10	0.2	3.75	66.31	65.52	49.74	50.72

Table 4. Independent variables and the observed and predicted values of Fe and Mn removal efficiencies by (CO-AC)

No	PH	Time	Adsorbent dose	Fe, Mn IN concentration	R3% observed	R3 % predicted	R4 % observed	R4 % predicted
1	6	50	2	3.75	80.31	79.32	83.02	81.62
2	6	30	0.2	0.5	79.48	78.97	72.94	73.99
3	4	10	1.1	3.75	77.68	77.17	51.82	52.87
4	8	30	1.1	7	79.77	79.54	74.72	77.25
5	6	30	2	0.5	79.88	79.37	73.14	74.19
6	8	10	1.1	3.75	78.48	77.97	85.9	86.95
7	6	50	0.2	3.75	87.52	86.49	72.61	73.23
8	4	30	1.1	7	79.93	79.96	64.57	61.98
9	6	50	1.1	0.5	81.28	82.57	78.4	78.9
10	6	10	1.1	7	78.45	77.9	71.77	71.55
11	8	30	0.2	3.75	79.51	80.04	82.64	79.21
12	4	30	0.2	3.75	79.53	79.8	60.05	61.74
13	8	30	2	3.75	79.97	80.44	82.05	80.64
14	4	30	2	3.75	80.21	80.42	64.2	67.9
15	6	30	1.1	3.75	88.53	88.53	77.51	77.51
16	6	50	1.1	7	81.03	81.77	72.32	72.6
17	4	30	1.1	0.5	78.79	78.79	68.14	64.29
18	8	30	1.1	0.5	79.73	79.47	77.98	79.24
19	6	10	2	3.75	80.89	81.7	73.78	71.83
20	6	10	0.2	3.75	72.76	73.52	72.56	72.63

Table 5. Independent variables and the observed and predicted values of iron and manganese removal efficiencies

No	PH	Time	Adsorbent dose	Fe, Mn IN concentration	R5% observed	R5 % predicted	R6 % observed	R6 % predicted
1	6	50	2	3.75	68.354	69.23	82.06	81.98
2	6	30	0.2	0.5	53.29	53.54	67.42	67.87
3	4	10	1.1	3.75	64.77	65.02	75.15	75.59
4	8	30	1.1	7	65.51	66.04	75.91	76.26
5	6	30	2	0.5	79	79.25	84.44	84.89
6	8	10	1.1	3.75	70.22	70.73	84.23	84.83
7	6	50	0.2	3.75	66.089	67.13	74.33	74.89
8	4	30	1.1	7	64.74	65.99	63.47	62.19
9	6	50	1.1	0.5	70.49	69.63	83.92	83.97
10	6	10	1.1	7	69.92	69.46	75.48	75.92
11	8	30	0.2	3.75	66.02	65.77	82.83	81.43
12	4	30	0.2	3.75	64.50	63.52	55.49	55.72
13	8	30	2	3.75	72.18	71.85	75.86	76.11
14	4	30	2	3.75	64.88	63.83	74.95	76.83
15	6	30	1.1	3.75	66	66	86.37	86.37
16	6	50	1.1	7	67.71	66.4	74.32	74.8
17	4	30	1.1	0.5	60.48	61.02	73.54	72.26
18	8	30	1.1	0.5	71.43	71.25	82.81	83.16
19	6	10	2	3.75	70.27	70.28	84.71	83.22
20	6	10	0.2	3.75	66.05	65.99	74.37	74.53

Table 6. ANOVA for analyze response surface models of Fe and Mn percent removals by (CI-AC)

Source	DF		Adj SS		Adj MS		F-Value		P-Value	
Source	R1	R2	R1	R2	R1	R2	R1	R2	R1	R2
Error	7	7	18.48	10.12	2.64	1.44				
Lack- of -fit	5	5	18.40	10.1	3.68	2.02	85.58	293.88	0.012	0.003
Pure error	2	2	0.086	0.01	0.04	0.007				
Total	21	21	332.52	808.14						

Table 7. ANOVA for analyze response surface models of Fe and Mn percent removals by (CO-AC)

Source	DF		Adj SS		Adj MS		F-Value		P-Value	
Source	R3	R4	R3	R4	R3	R4	R3	R4	R3	R4
Error	7	7	9.81	78.47	1.4	11.21				
Lack- of -fit	5	5	9.452	76.18	1.8904	15.236	10.30	13.28	0.091	0.072
Pure error	2	2	0.367	2.29	0.1836	1.147				
Total	21	21	199.337	1529.76						

Table 8. ANOVA for analyze response surface models of Fe and Mn percent removals by (LU-AC)

Source	DF		Adj SS		Adj MS		F-Value		P-Value	
Source	R5	R6	R5	R6	R5	R6	R5	R6	R5	R6
Error	7	7	9.53	14.14	1.36	2.02				
Lack- of -fit	5	5	9.02	13.41	1.80	2.68	7.07	7.34	.128	.124
Pure error	2	2	0.51	0.73	0.255	0.365				
Total	21	21	508.89	1277.86						

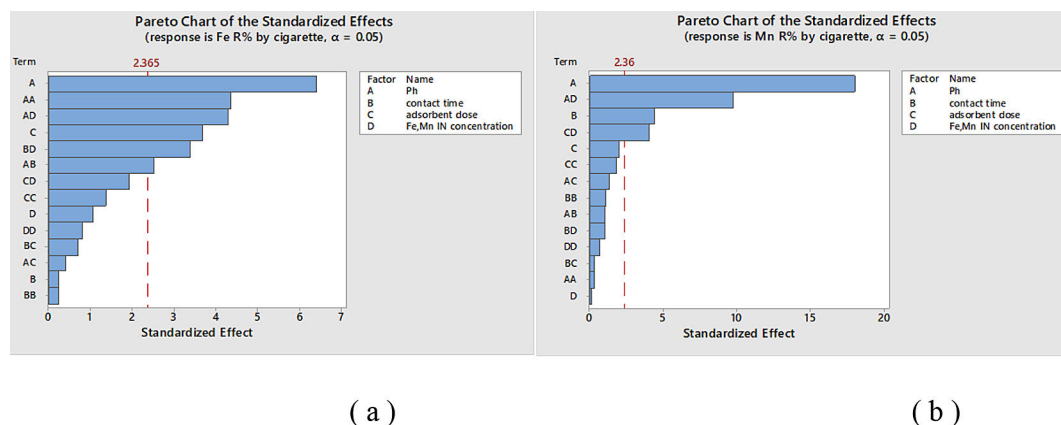


Figure 5. Pareto charts for each operating model to display (a) percentage of iron removal and (b) percentage of manganese removal by (CI-AC)

9, 11, and 13 for manganese removal (R%) illustrate the relationship and impact of four factors (pH, contact time, adsorbent dose, and initial Fe/Mn concentration) on removal efficiency. These response plots, generated from the quadratic model using Minitab®18 software, assess the effect of variable interactions by displaying the response as two variables are varied within the experimental

range while the other two are held constant. Cigarette butts activated carbon effectively removes iron and manganese, with removal efficiency increasing significantly with pH and contact time. Maximum iron removal (72.4%) occurred at pH 7.2 and 50 minutes contact time (Figure 8a), while maximum manganese removal (62%) occurred at pH 8 and 50 minutes (Figure 9a).

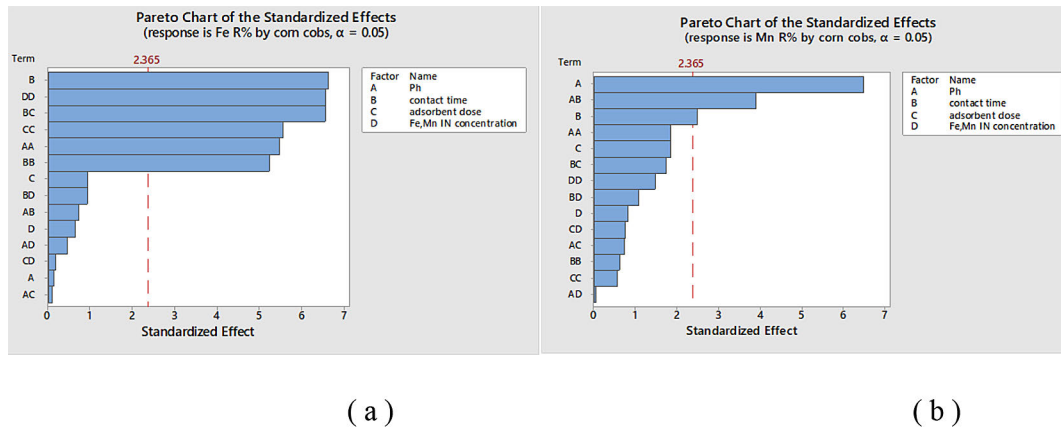


Figure 6. Pareto charts for each operating model to display (a) percentage of iron removal and (b) percentage of manganese removal by (CO-AC)

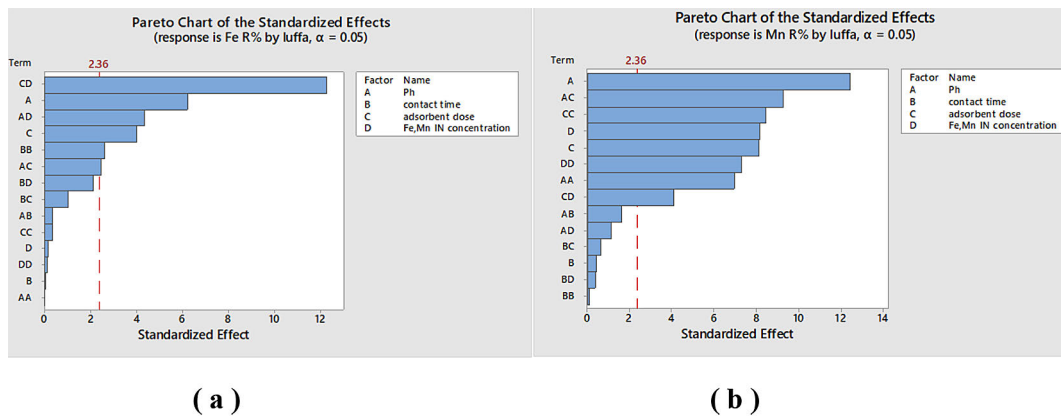


Figure 7. Pareto charts for each operating model to display (a) percentage of iron removal and (b) percentage of manganese removal by (LU-AC)

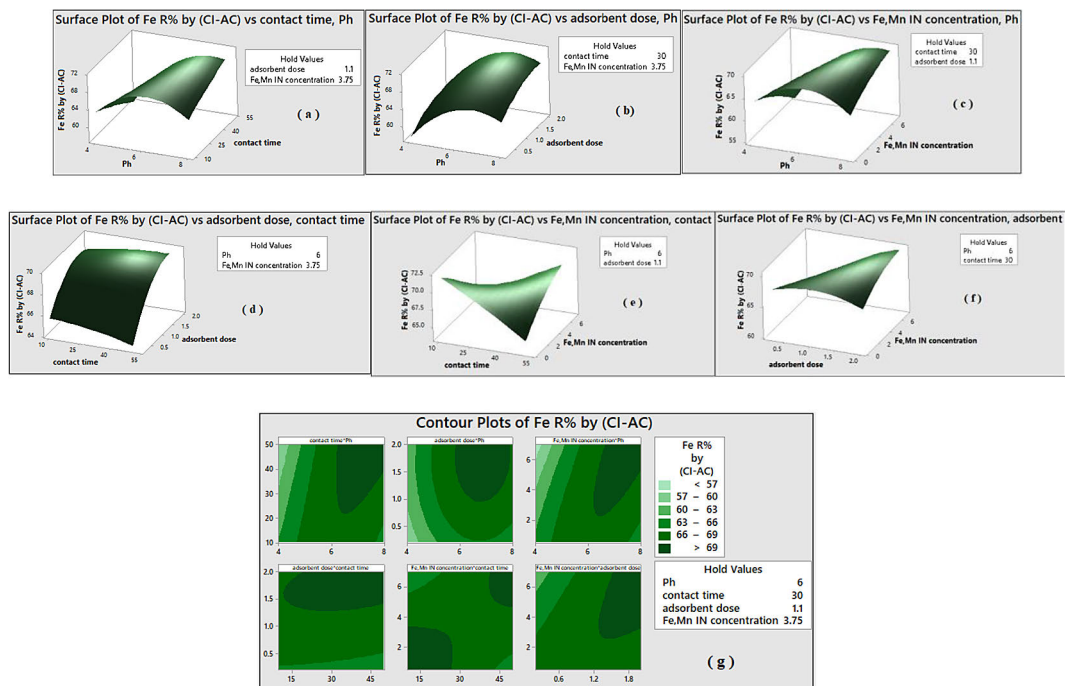


Figure 8. Surface plots and contour plots for iron removal efficiency by (CI-AC)

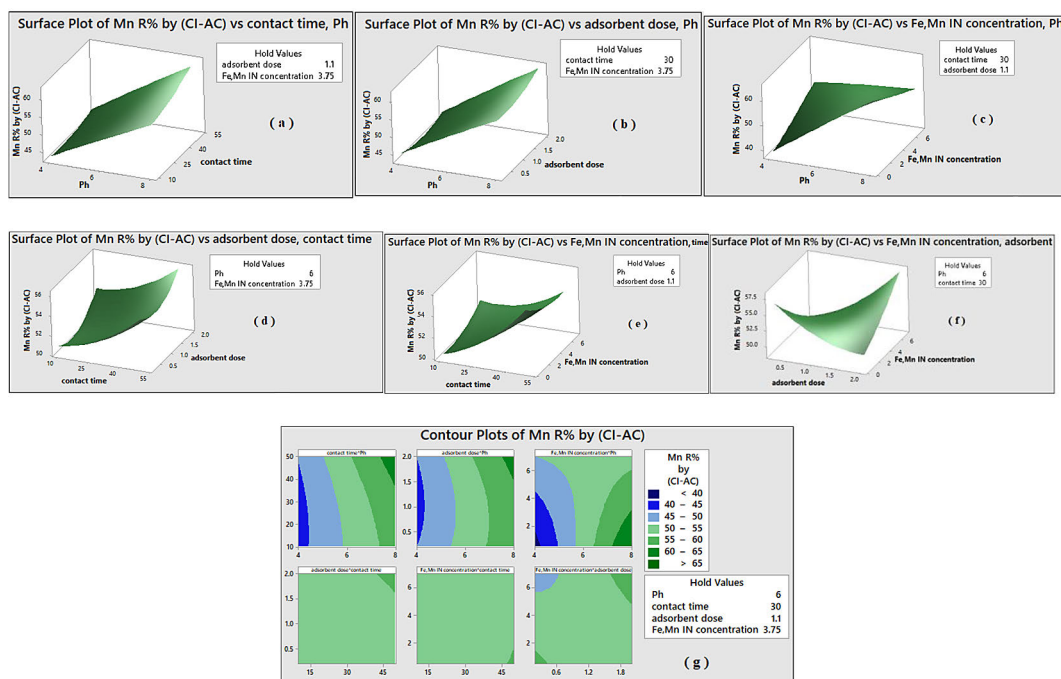


Figure 9. Surface plots and contour plots for manganese removal efficiency by (CI-AC)

Higher pH and larger adsorbent doses improved Fe and Mn removal. Maximum removal rates were 70% for Fe at pH 7.5 and a 2 g adsorbent dose, and 61.5% for Mn at pH 8 and a 2 g adsorbent dose (Figure 8b and 9b). Increased initial Fe and Mn concentrations reduced removal efficiency, but this effect was mitigated by higher pH (Figure 8c and 9c).

Increasing contact time and adsorbent dose enhanced both Fe and Mn removal. Maximum Fe removal (69%) occurred within a contact time of 10–50 min and an adsorbent dose of 1.2–2 g. Similarly, Mn removal efficiency increased with both contact time and adsorbent dose, reaching a maximum of 55% at 50 minutes and 2 g, as shown in Figure 8d and Figure 9d.

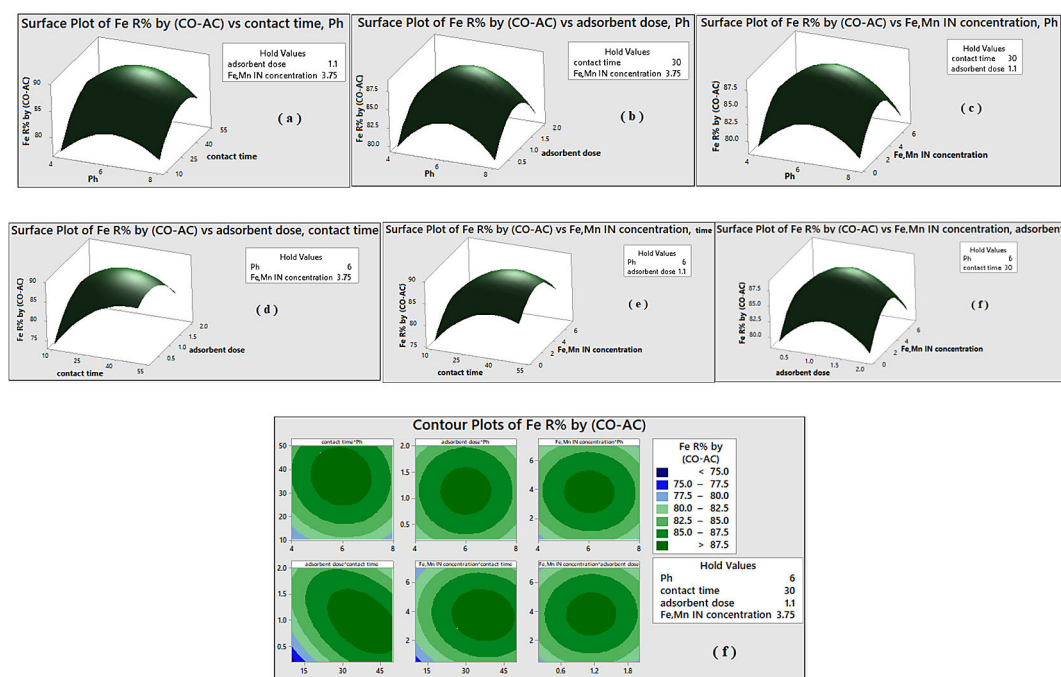


Figure 10. Surface plots and contour plots for Fe removal efficiency by (CO-AC)

Iron and manganese removal increased with longer contact times but decreased with higher concentrations as shown in Figure 8e and Figure 9e. As shown in Figures 8f and 9f, higher doses and lower concentrations improved iron and manganese removal. The highest removal efficiencies were 69% for iron and 55% for manganese, both achieved at a 1.0 g dose and low initial concentrations. Corn cob activated carbon effectively removes both iron and manganese, with removal efficiency increasing alongside pH and contact time. Maximum removal efficiencies were achieved at approximately pH 7.2 and 50 minutes (89.2% for iron, Figure 10a; 85% for manganese at pH 7, Figure 11a).

Iron and manganese removal improved with increasing pH and adsorbent dose, demonstrating a synergistic effect. Maximum removal efficiencies of 88.6% for iron and 85.4% for manganese were achieved at pH 7.3 and an adsorbent dose of 1.0 g (Figure 10b and 11b). Removal efficiency increased at lower initial iron and manganese concentrations and higher pH levels (Figure 10c and 11c).

Iron and manganese removal efficiency increased with contact time and adsorbent dose, reaching maxima of 89.7% and 86.5%, respectively, at 55 minutes and 1.0 g (Figures 10d and 11d). Longer contact times improved iron removal, while higher initial concentrations reduced efficiency; maximum iron removal was 87.1% at 60 minutes with low initial concentration (Figures

10e and 11e). Similarly, manganese removal increased with time but decreased with higher initial concentrations, peaking at 76.2% at 60 minutes with low concentration (Figures 10e and 11e). Iron and manganese removal increased with higher adsorbent dose and decreased with higher initial concentrations (Figures 10f and 11f).

Luffa sponge activated carbon effectively removes iron and manganese. Figures 12a and 13(a) indicate that removal efficiency for both metals increases with pH and contact time, with maximum removal exceeding 75% for iron (pH 6.5–7.5, 50 minutes) and 85% for manganese (pH 7.5, 55 minutes). As shown in Figures 12(b) and 13b, increasing both pH and adsorbent dose enhances removal. Peak removal occurred at pH 7.3 and a 1.0 g dose, reaching 81% for iron and 87.9% for manganese. Figures 12c and 13c illustrate that higher pH levels counteract the decrease in removal efficiency observed with increasing initial concentrations. Contact time and adsorbent dose positively impact removal, with maximum removal of 87.6% for iron and 82.4% for manganese achieved at 55 minutes and a 1.5 g dose (Figures 12d and 13d). Figures 12e and 13e show that while removal slightly decreases with higher concentrations, longer contact times improve performance. Higher adsorbent doses, especially at low initial concentrations, also improve removal, reaching 87.8% for iron and 85.4% for manganese at a 1.2 g dose.

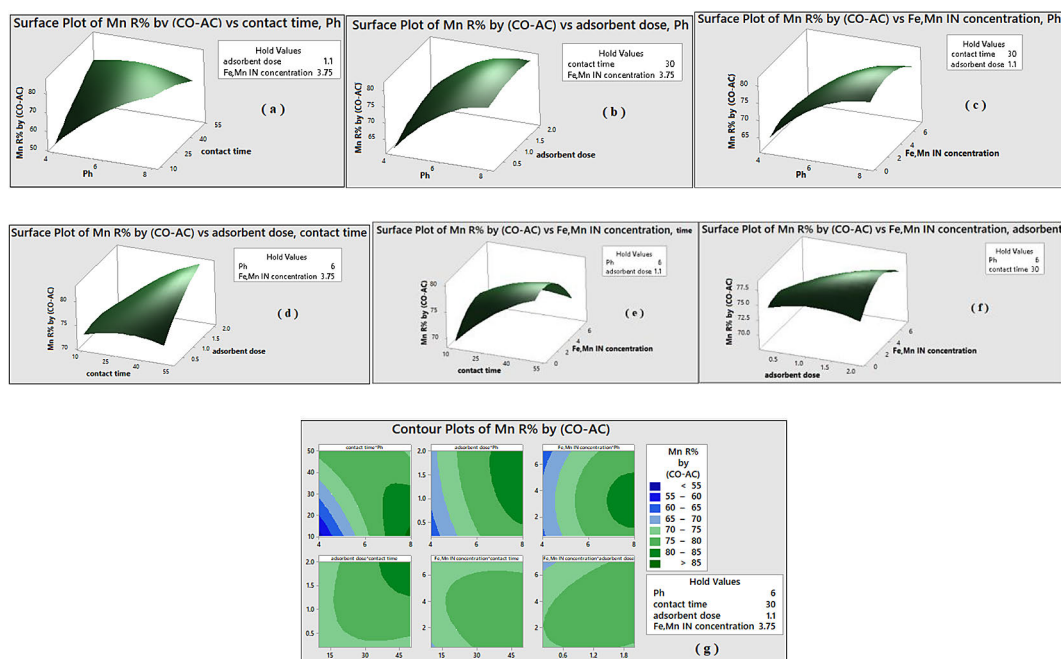


Figure 11. Surface plots and contour plots for Mn removal efficiency by (CO-AC)

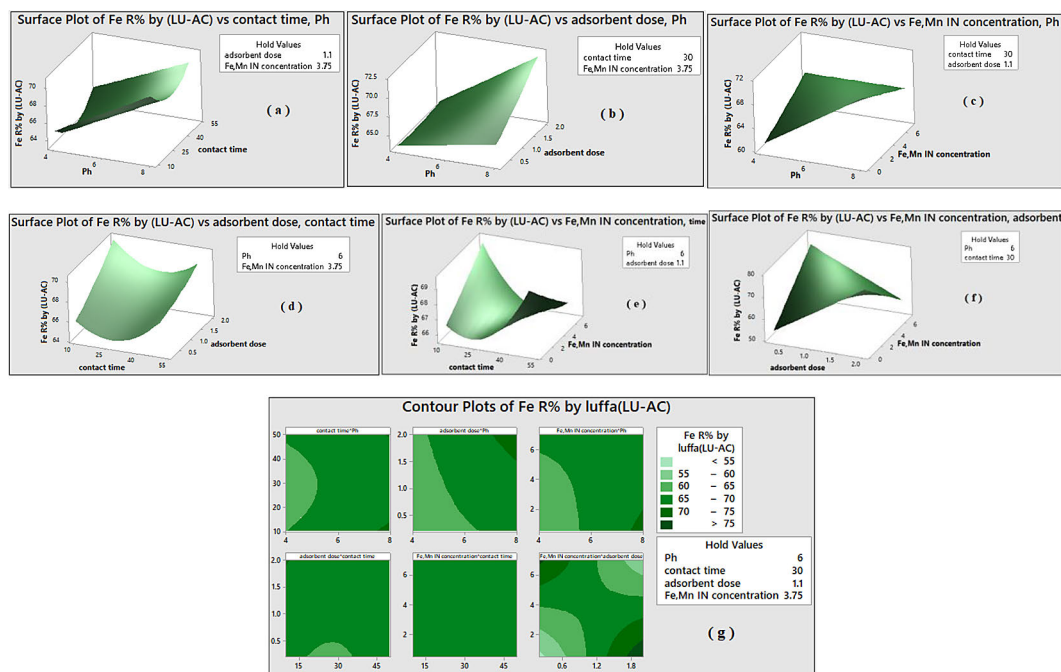


Figure 12. Surface plots and contour plots of iron removal efficiency by (LU-AC)

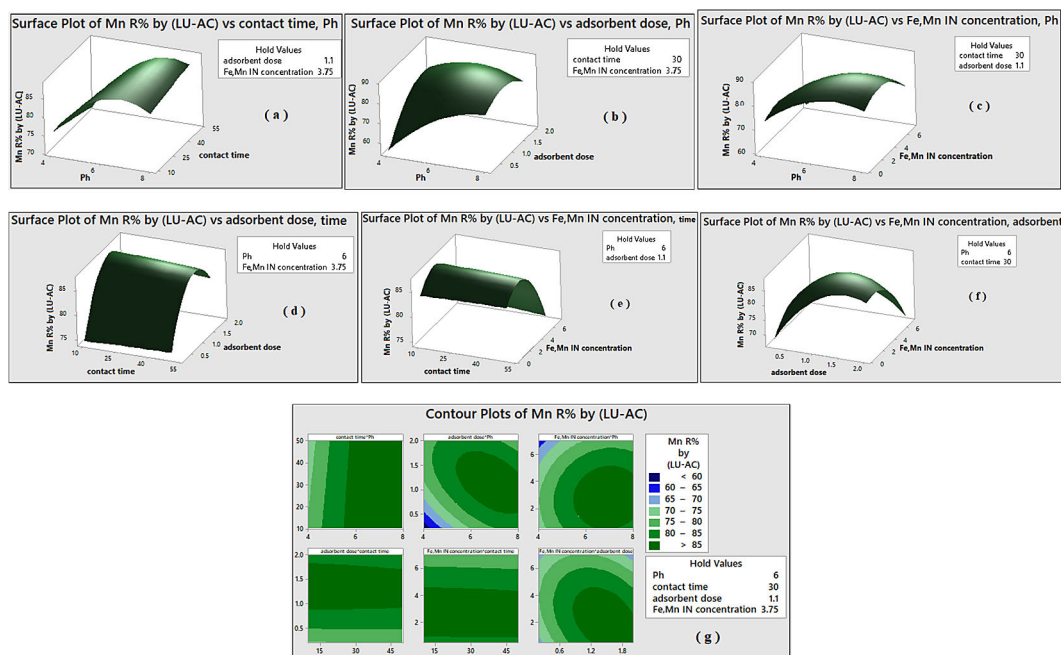


Figure 13. Surface plots and contour plots of manganese removal efficiency by (LU-AC)

Optimization of the Fe and Mn removal efficiencies by cigarette butts, corn cobs and luffa sponge activated carbon

Minitab®18's response optimizer determined optimal conditions for pH, contact time, adsorbent dose, and initial Fe/Mn concentration. D-optimization penalties are shown in Figure 14. For (CI-AC), optimal removal efficiencies

were 70.3% for iron and 65.12% for manganese, achieved at pH 8, 50 minutes contact time, a 2 gram adsorbent dose, and 3.32 mg/L initial Fe/Mn concentration. For (CO-AC) (Figure 15), optimal removal efficiencies were 88.53% for iron and 79.57% for manganese, achieved at pH 6.34, 37.87 minutes contact time, a 1.25 gram adsorbent dose, and 3.5 mg/L initial Fe/Mn concentration. For (LU-AC) (Figure 16), optimal removal

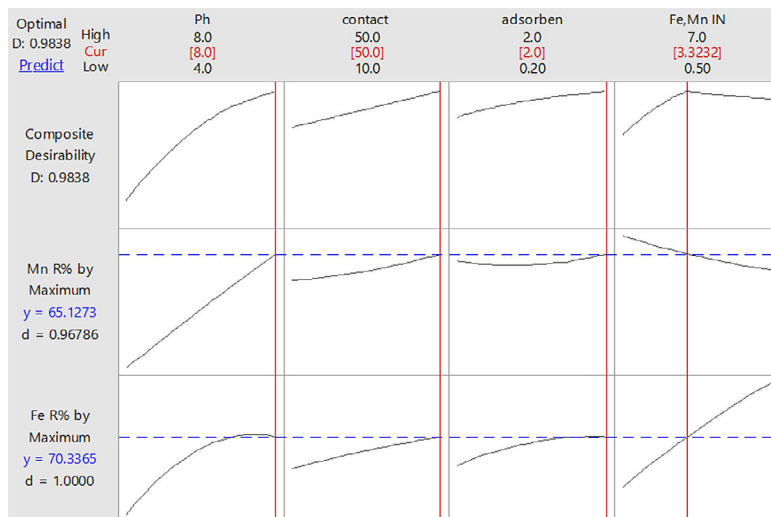


Figure 14. Optimization of operating parameters for maximum removal of Fe and Mn by (CI-AC)

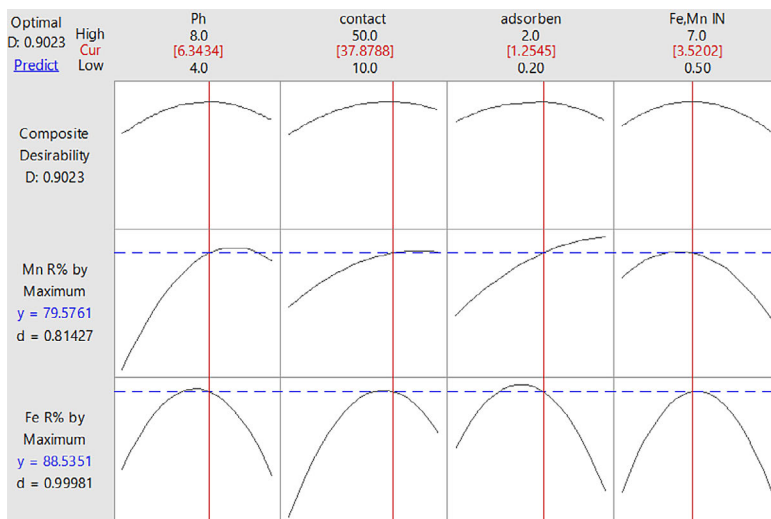


Figure 15. Optimization of operating parameters for maximum removal of Fe and Mn by (CO-AC)

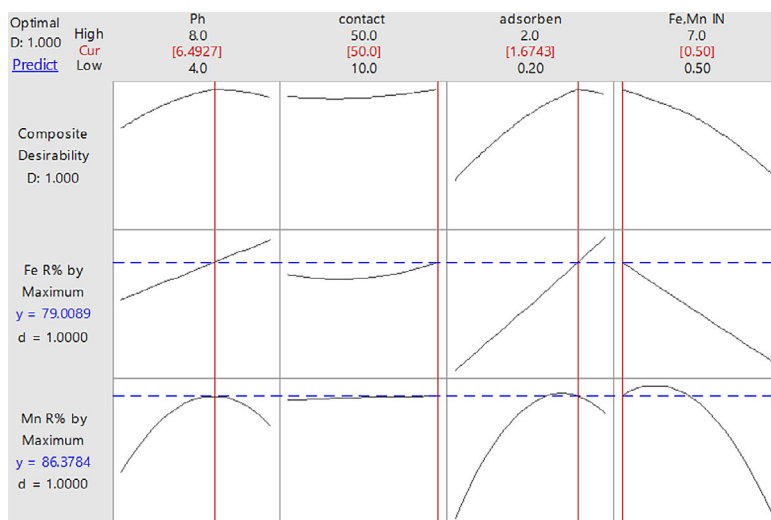


Figure 16. Optimization of operating parameters for maximum removal of Fe and Mn by (LU-AC)

efficiencies were 79.008% for iron and 86.37% for manganese, achieved at pH 6.49, 50 minutes contact time, a 1.67 gram adsorbent dose, and 0.5 mg/L initial Fe/Mn concentration.

CONCLUSIONS

This study evaluated the effectiveness of activated carbon derived from cigarette butts (CI-AC), corn cobs (CO-AC), and luffa sponge (LU-AC) in removing Fe and Mn from contaminated groundwater. FTIR analysis confirmed the involvement of functional groups (O-H, C=O, C-O) in adsorption. Response Surface Methodology (RSM) was used to investigate the interaction of pH, Fe and Mn initial concentration, contact time, and adsorbent dose, successfully optimizing operational parameters with high R^2 values (94.44–98.89), validating the model's reliability. Pareto charts identified pH and adsorbent dose as the most influential factors. CO-AC exhibited the highest removal efficiencies (88.53% for Fe and 79.75% for Mn) under optimal conditions (pH 6.34, 37.8 minutes, 1.25 g, 3.52 mg/l), followed by LU-AC (79% for Fe and 86.37% for Mn) at pH 6.49, 50 minutes, 1.67 g, and 0.5 mg/l. CI-AC showed the lowest efficiency (70.33% Fe and 65.12% Mn removal) at pH 8, 50 minutes, 2 g, and 3.32 mg/l. Higher pH levels significantly enhanced Fe and Mn adsorption for all adsorbents. Longer contact times (up to 50 minutes) improved removal efficiencies, and increased adsorbent dosage correlated with higher removal rates. Lower initial concentrations of Fe and Mn resulted in higher removal efficiencies.

REFERENCES

- Akbar, A., Abdul Aziz, H., Adlan, N. (2016). *Potential of high quality limestone as adsorbent for iron and manganese removal in groundwater*. www.jurnalteknologi.utm.my
- Akbari Zadeh, M., Dagbandan, A., Abbasi Souraki, B. (2022). Removal of iron and manganese from groundwater sources using nano-biosorbents. *Chemical and Biological Technologies in Agriculture*, 9(1). <https://doi.org/10.1186/s40538-021-00268-x>
- Anastopoulos, I., Robalds, A., Tran, H. N., Mitrogiannis, D., Giannakoudakis, D. A., Hosseini-Bandegharai, A., Dotto, G. L. (2019). Removal of heavy metals by leaves-derived biosorbents. In *Environmental Chemistry Letters* 17(2), 755–766. Springer
- Barloková, D., Ilavský, J. (2010). Introduction Removal of Iron and Manganese from Water Using Filtration by Natural Materials. In *Polish J. of Environ. Stud* 19, (6).
- El-Haddad, M. N. (2013). Chitosan as a green inhibitor for copper corrosion in acidic medium. *International Journal of Biological Macromolecules*, 55, 142–149. <https://doi.org/10.1016/j.ijbiomac.2012.12.044>
- El-Haddad, M. N. (2020). Spectroscopic, electrochemical and quantum chemical studies for adsorption action of polyethylene oxide on copper surface in NaCl solution. *Zeitschrift Fur Physikalische Chemie*, 234(11), 1835–1851. <https://doi.org/10.1515/zpch-2019-1390>
- Krishni, R. R., Foo, K. Y., Hameed, B. H. (2014). Adsorptive removal of methylene blue using the natural adsorbent-banana leaves. *Desalination and Water Treatment*, 52(31–33), 6104–6112. <https://doi.org/10.1080/19443994.2013.815687>
- Mahmoud, M. S., Ahmed, S. M., Mohammad, S. G., Abou Elmagd, A. M. (2014). Evaluation of Egyptian banana peel (*Musa* sp.) as a green sorbent for groundwater treatment. *International Journal of Engineering and Technology*, 4(11).
- Mani, D., & Kumar, C. (2014). Biotechnological advances in bioremediation of heavy metals contaminated ecosystems: An overview with special reference to phytoremediation. In *International Journal of Environmental Science and Technology* 11(3), 843–872. Center for Environmental and Energy Research and Studies. <https://doi.org/10.1007/s13762-013-0299-8>
- Matouq, M., Jildeh, N., Qtaishat, M., Hindiyeh, M., Al Syouf, M. Q. (2015). The adsorption kinetics and modeling for heavy metals removal from wastewater by Moringa pods. *Journal of Environmental Chemical Engineering*, 3(2), 775–784. <https://doi.org/10.1016/j.jece.2015.03.027>
- Nandiyanto, A. B. D., Ragadhita, R., Fiandini, M. (2023). Interpretation of fourier transform infrared spectra (FTIR): A practical approach in the polymer/plastic thermal decomposition. *Indonesian Journal of Science and Technology*, 8(1), 113–126. <https://doi.org/10.17509/ijost.v8i1.53297>
- Overview, F. (2016). *EJCHEM-Volume 59-Issue 3-Page 321-362*. 362(3), 321–362.
- Pereira, L. M. S., Milan, T. M., Tapia-Blácido, D. R. (2021). Using response surface methodology (RSM) to optimize 2G bioethanol production: A review. In *Biomass and Bioenergy* 151. Elsevier Ltd. <https://doi.org/10.1016/j.biombioe.2021.106166>
- Singh, B., Kumar, R., Ahuja, N. (2005). Optimizing drug delivery systems using systematic “design of

- experiments.” Part I: Fundamental aspects. In *Critical Reviews in Therapeutic Drug Carrier Systems* 22(1), 27–105. <https://doi.org/10.1615/CritRevTherDrugCarrierSyst.v22.i1.20>
15. Su, J. F., Huang, Z., Yuan, X. Y., Wang, X. Y., Li, M. (2010). Structure and properties of carboxymethyl cellulose/soy protein isolate blend edible films crosslinked by Maillard reactions. *Carbohydrate Polymers*, 79(1), 145–153. <https://doi.org/10.1016/j.carbpol.2009.07.035>
16. Thinojah, T., Ketheesan, B. (2022). Iron removal from groundwater using granular activated carbon filters by oxidation coupled with the adsorption process. *Journal of Water and Climate Change*, 13(5), 1985–1994. <https://doi.org/10.2166/wcc.2022.126>
17. Wang, X. S., Tang, Y. P., Tao, S. R. (2009). Kinetics, equilibrium and thermodynamic study on removal of Cr (VI) from aqueous solutions using low-cost adsorbent Alligator weed. *Chemical Engineering Journal*, 148(2–3), 217–225. <https://doi.org/10.1016/j.cej.2008.08.020>
18. Zhao, M., Xu, Y., Zhang, C., Rong, H., Zeng, G. (2016). New trends in removing heavy metals from wastewater. In *Applied Microbiology and Biotechnology* 100(15), 6509–6518. Springer Verlag. <https://doi.org/10.1007/s00253-016-7646-x>